Quantum chaos and critical behavior on a chip

Neill Lambert,[1] Yueh-nan Chen,[2] Robert Johansson,[1] and Franco Nori[1,3]
[1]*Advanced Science Institute, The Institute of Physical and Chemical Research (RIKEN), Saitama 351-0198, Japan*
[2]*Department of Physics and National Center for Theoretical Sciences, National Cheng-Kung University, Tainan 701, Taiwan*
[3]*Center for Theoretical Physics, Physics Department, Applied Physics Program, Center for the Study of Complex Systems, The University of Michigan, Ann Arbor, Michigan 48109-1040, USA*
(Received 8 June 2009; published 6 October 2009)

The Dicke model describes N qubits (or two-level atoms) homogeneously coupled to a bosonic mode. Here we examine an open-system realization of the Dicke model, which contains critical and chaotic behaviors. In particular, we extend this model to include an additional open transport qubit (coupled to the bosonic mode) for passive and active measurements. We illustrate how the scaling (in the number of qubits N) of the super-radiant phase transition can be observed in both current and current-noise measurements through the transport qubit. Using a master equation, we also investigate how the phase transition is affected by the back action from the transport qubit and losses in the cavity. In addition, we show that the nonintegrable quantum chaotic character of the Dicke model is retained in an open-system environment. We propose how all of these effects could been seen in a circuit-QED system formed from an array of superconducting qubits, or an atom chip, coupled to a quantized resonant cavity (e.g., a microwave transmission line).

DOI: 10.1103/PhysRevB.80.165308 PACS number(s): 64.70.Tg, 42.50.Ct, 05.45.Mt

I. INTRODUCTION

Understanding and categorizing complex modes of behavior, such as quantum phase transitions[1] and quantum chaos,[2] is an important part of quantum many-body theory. Recently, concepts and formalisms from quantum information theory have been used to understand and classify several aspects of criticality.[3–7] However, the realization of strong-coupling regimes, coherent dynamics, and careful readout necessary to observe these phenomena in laboratory conditions is challenging.

Our goal here is to show how a particular quantum phase transition, the Dicke super-radiant transition[7–9] behaves when coupled to the environment and measured using transport techniques, as is the case in realistic experimental conditions. The Dicke model describes N two-level "atoms" or qubits coupled to a common single-mode cavity. We focus on this model because of the recent advances in on-chip "circuit QED,"[10–18] where the strong-coupling regime is accessible and which allow for coupling to a range of artificial atoms and measurement apparatuses. In particular, we propose a dispersive measurement scheme to observe this transition by coupling either a superconducting qubit array or an atom chip, to a cavity which is simultaneously (dispersively) coupled to a nonequilibrium measurement device (a so-called *"transport" qubit*[19]), realizable with a superconducting single electron transistor, or double quantum dot. The geometry of the proposed device is shown in Fig. 1 and described in detail in its caption.

We begin by outlining the salient features of the phase transition in the Dicke model, and existing work in this area (Sec. II), and discussing the closed (Sec. III) and open (Sec. IV) descriptions of the model. We then investigate how coupling to a transport qubit (TQ) allows readout of the phase-transition properties and give analytical and numerical results for the current and current noise in the zero back-action limit (Sec. V). We then discuss our main result that the current can be used as an *observable order parameter* to detect the phase transition (Sec. VI). This complements a recent surge of interest in identifying signatures of complex behavior in mesoscopic transport measurements.[19–21] We then consider back-action and decoherence (cavity-loss) effects using a master-equation approach (Sec. VII). We show that both transport qubit back action and cavity loss appear to only have a weak affect on the current measurement near the critical point. In addition, we show that the Liouvillian describ-

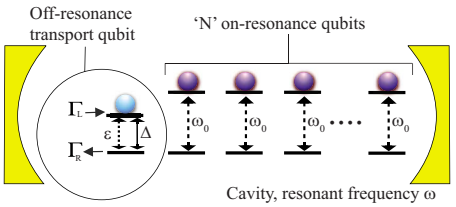

FIG. 1. (Color online) Geometry of the proposed device. N qubits are placed at the antinode(s) of a "cavity" with resonant frequency ω (depending on specific realization, they might alternatively be placed at one antinode, or at subsequent antinodes, to minimize qubit-qubit interactions). Their energy splittings are on-resonance with the oscillator $\omega_0=\omega$. An additional "open" TQ (shown in the left) is also coupled to the cavity off-resonance ($\epsilon \neq \omega$) and used to passively readout the state of the cavity mode. In the figure, the solid lines represent tunneling while the dashed lines represent energy gaps. The properties of the transport qubit are defined by an energy splitting ϵ, coherent tunneling rate Δ and transport rates Γ_L and Γ_R. In addition, the cavity mode has a cavity decay rate γ_b, not shown in the figure. Superconducting artificial atoms coupled to an on-chip cavity (e.g., a quantized LC oscillator or microwave transmission line) are a feasible realization using current technology. The transport qubit can be realized using a charge qubit in the transport regime, i.e., a superconducting single electron transistor. Alternatively, a large number of qubits in the form of two-level atoms in an atom chip, coupled to a transmission line, has recently been proposed as a way to realize the large-N Dicke model (Ref. 22).

ing the open-system dynamics has an eigenvalue spectrum similar to that of the Wigner–Dyson distribution of random matrix theory, as in the closed system case (Sec. VIII). Finally, we briefly discuss practical schemes to realize this model in an experiment[10–16,22] (Sec. IX).

The measurement scheme we are proposing is based on charge transport through an effective qubit. Such systems are well known to be highly sensitive detectors (electrometers) but associated with the charge transport process is a large back action on the system being detected. This is due to the stochastic nature of the transport process.[23] An alternative to the transport scheme we propose here would be doing transmission spectroscopy on the cavity/resonator itself.[24] Another possibility, in the same spirit as our dispersive transport qubit, would be using an additional off-resonance superconducting charge or phase qubit coupled to the cavity, which is then probed using an appropriate qubit-spectroscopy scheme.[25]

We point out that the properties we investigate here require the precise control of the couplings between qubits and the resonator, and access to a very strong-coupling regime. Fortunately, recent work has shown that this ultrastrong-coupling regime, where the Jaynes–Cummings approximation no longer holds, is now accessible for circuit-QED systems.[26] Furthermore, in such systems the coupling strength can be tuned by biasing the qubits away from the degeneracy point or by tuning them off-resonance by applying ac stark or Zeeman shifts, thus reducing the effective interaction.[27,28]

In addition, it was recently shown[29] that the generalized Dicke model, a variation in the Dicke model where the couplings between the N qubits and the cavity are inhomogeneous, still has all the critical properties of the standard Dicke model. This indicates the universality of the Dicke phase transition, as well as making an experimental realization more feasible. Furthermore, a realization using Raman transitions in atoms in an optical cavity has also been proposed as a method to reach a controllable strong-coupling regime.[24]

II. DICKE SUPERRADIANT PHASE TRANSITION

Historically, the Dicke Hamiltonian describes the dipole interaction between N atoms and n_b bosonic field modes. Typically[30] the atoms are considered to be at fixed sites within a cavity of volume V. The atoms are assumed to be well separated and thus noninteracting. Hereafter we refer to the atoms as "qubits" and the additional measurement qubit as the "transport qubit." To observe critical phenomena we consider the single-mode case. We do not make the rotating wave approximation, allowing the model to describe both weak- and strong-coupling regimes (and we omit the $\hat{A}^2$ term).

Previous work[7,9] on this model has shown an exact analytical solution in the limit $N\to\infty$. Furthermore, the transition was characterized as a breaking of parity symmetry at a particular value of the coupling between qubits and cavity (denoted by λ, with the critical value being λ_c). Both the qubits and the cavity bosonic degrees of freedom become "macroscopically occupied" (i.e., of $O(N)$, the number of qubits) in the regime above the critical point $\lambda>\lambda_c$. For finite arrays of qubits, N, the system is known to exhibit power-law scaling,[31] quantum chaos,[9] and critical entanglement.[7,32]

Several proposals for an experimental realization of this system have already been made. For example, Dimer *et al.*[24] proposed a cavity QED realization and discussed in detail the effect of the cavity decay on the phase transition. In another work, Chen *et al.*[27] proposed using superconducting charge qubits coupled to an optical cavity so that the critical properties can be observed in the optical mode using heterodyne detection. In addition they proposed observing the phase transition as a function of level splitting, rather than coupling strength.

III. DICKE HAMILTONIAN

The single-mode Dicke Hamiltonian is defined as

$$H_D = \omega_0 \sum_{i=1}^{N} s_z^{(i)} + \omega a^\dagger a + \sum_{i=1}^{N} \frac{\lambda}{\sqrt{N}}(a^\dagger + a)(s_+^{(i)} + s_-^{(i)})$$

$$= \omega_0 J_z + \omega a^\dagger a + \frac{\lambda}{\sqrt{N}}(a^\dagger + a)(J_+ + J_-), \tag{1}$$

where $J_z=\Sigma_{i=1}^N s_z^i$ and $J_\pm=\Sigma_{i=1}^N s_\pm^i$ are collective angular momentum operators for a pseudospin of length $j=N/2$. These operators obey the usual angular momentum commutation relations, $[J_z,J_\pm]=\pm J_\pm$ and $[J_+,J_-]=2J_z$. The frequency ω_0 describes the qubit level splitting, ω is the oscillator field frequency, and λ the qubit-field coupling strength. Because of their mutual interaction with the oscillator field the qubits are not independent. The $\lambda/\sqrt{N}$ scaling is important to realize the thermodynamic limit. It essentially bosonizes the low-energy part of the state space of the collective angular momentum. Physically, this scaling implies that the density of qubits is constant so that the cavity volume becomes larger as N is increased, consequently reducing the electric field density and thus the effective interaction with each individual qubit.

First, we will show analytical results for an entirely passive measurement of the system, using an off-resonance ancillary qubit with current transport. Second, we will treat the back action of the ancillary qubit as a fully quantum interaction, with Markovian transport properties, and including decay terms for the cavity. We will see how this alters the final current measurements, as well as how it changes the properties of the phase transition.

IV. MASTER EQUATION

To take into account the back action of the transport qubit on the Dicke Hamiltonian, we can model the whole system using a master equation,

$$\frac{d}{dt}\rho(t) = L[\rho(t)] = -i[H,\rho(t)] + L_0[\rho(t)],$$

$$H = H_D + H_{\mathrm{TQ}} + H_{\mathrm{int}}, \quad L_0 = L_{\mathrm{TQ}} + L_C, \tag{2}$$

where

$$H_{\mathrm{TQ}} = \epsilon\sigma_z + \Delta\sigma_x \tag{3}$$

is the Hamiltonian of the transport qubit where ϵ is the level splitting and Δ the coherent tunneling within the TQ,

$$H_{\mathrm{int}} = g\sigma_z a^\dagger a \tag{4}$$

is the off-resonance dispersive interaction between Dicke system and TQ. The coupling g is actually second order in the true cavity-TQ coupling, see, for example, Blais *et al.*[33] The term L_{TQ} contains the transport properties of the TQ[19] and L_C contains cavity damping terms (e.g., photons leaking from the cavity),

$$L_{\mathrm{TQ}}[\rho(t)] = -\frac{\Gamma_L}{2}[s_L s_L^\dagger \rho(t) - 2s_L^\dagger \rho(t) s_L + \rho(t) s_L s_L^\dagger] - \frac{\Gamma_R}{2}[s_R^\dagger s_R \rho(t) - 2 s_R \rho(t) s_R^\dagger + \rho(t) s_R^\dagger s_R], \tag{5}$$

$$L_C = -\frac{\gamma_b}{2}[a^\dagger a \rho - 2a\rho a^\dagger + \rho a^\dagger a], \tag{6}$$

where

$$s_L = |0\rangle\langle L|, \quad s_L^\dagger = |L\rangle\langle 0|, \tag{7}$$

$$s_R = |0\rangle\langle R|, \quad s_R^\dagger = |R\rangle\langle 0|, \tag{8}$$

Γ_L and Γ_R are the left/right tunneling rates for the TQ and γ_b is the decay rate of photons out of the cavity (throughout, we set $\hbar = 1$). Here $\rho(t)$ is the density matrix describing the state of the qubit-array, cavity, and transport qubit system.

V. PASSIVE MEASUREMENT

If we assume no back action from the transport qubit onto the Dicke model, the problem is very simple. However, the form of the interaction between the transport qubit and the effective cavity is still important. As mentioned, off-resonance, $\epsilon \ll \omega$, we assume the interaction is dispersive,[25] $H_{\mathrm{int}} = g\sigma_z a^\dagger a$. For an entirely nondestructive passive measurement (with no feedback), the state of the ancillary transport qubit is then just shifted by the occupation of the transmission line [i.e., considering the mean field of Eq. (3)],

$$H_{\mathrm{TQ}} \approx (\epsilon + g\langle a^\dagger a\rangle)\sigma_z + \Delta\sigma_x. \tag{9}$$

We are able to calculate the analytical values of $\langle a^\dagger a\rangle$ in the limit $N \to \infty$. The transport properties are easily calculated using a counting-statistics approach, which has been well summarized elsewhere.[19] Thus, the current and zero-frequency current noise measured through the ancillary qubit is simply given by

$$\frac{I}{e} = \frac{\Delta^2 \Gamma_R}{\Delta^2(2 + \Gamma_L/\Gamma_R) + \Gamma_R^2/4 + (\epsilon + g\langle a^\dagger a\rangle)^2}, \tag{10}$$

$$S(0) = 2eI\left\{1 - 8\Gamma_L\Delta^2 \frac{4(\epsilon + g\langle a^\dagger a\rangle)^2(\Gamma_R - \Gamma_L) + \Gamma_R(3\Gamma_L\Gamma_R + \Gamma_R^2 + 8\Delta^2)}{[4\Delta^2(2\Gamma_L + \Gamma_R) + \Gamma_L\Gamma_R^2 + 4(\epsilon + g\langle a^\dagger a\rangle)^2\Gamma_L]^2}\right\}. \tag{11}$$

In the limit $N \to \infty$ the Dicke Hamiltonian has two distinct solutions, corresponding to the two phases of the transition. In the super-radiant phase both cavity and qubit array have a macroscopic mean-field displacement.

In the lower, "normal phase," we define the occupation of the cavity $\langle a^\dagger a\rangle$ by an effective temperature T and frequency Ω,

$$\langle a^\dagger a\rangle = \left(\frac{m\Omega}{4\omega} + \frac{\omega}{4m\Omega}\right)\coth\left(\frac{\Omega}{2T}\right) - \frac{1}{2}, \tag{12}$$

where Ω and T depend on the eigenenergies of H,

$$[\epsilon_\pm^{(1)}]^2 = \frac{1}{2}(\omega^2 + \omega_0^2 \pm \sqrt{(\omega_0^2 - \omega^2)^2 + 16\lambda^2\omega\omega_0}), \tag{13}$$

where ϵ_- is only real for $\lambda \leq \lambda_c$, giving the range of this solution. The dependence of T and Ω on the eigenvalues is via the relations,

$$\cosh\beta\Omega = \left[1 + \frac{2\epsilon_-\epsilon_+}{(\epsilon_- - \epsilon_+)^2 c^2 s^2}\right], \tag{14}$$

$$m\Omega = \left\{\left[1 + \frac{2\epsilon_-\epsilon_+}{(\epsilon_- - \epsilon+)^2 c^2 s^2}\right]^2 - 1\right\}^{1/2} \tag{15}$$

$$\times \left[\frac{(\epsilon_- - \epsilon_+)^2 c^2 s^2}{2(\epsilon_- s^2 + \epsilon_+ c^2)}\right], \tag{16}$$

$$c \equiv \cos\gamma^{(1)}, \quad s \equiv \sin\gamma^{(1)}, \tag{17}$$

$$\tan(2\gamma^{(1)}) = \frac{4\lambda\sqrt{\omega\omega_0}}{(\omega_0^2 - \omega^2)}, \tag{18}$$

where $\beta = 1/k_B T$. These define two equations linking the three parameters of the cavity/qubit system ω, ω_0, and λ, and the three effective parameters of a thermal oscillator β, Ω,

and m. By setting one energy scale of the original system such that $\omega=1$ and that of the thermal oscillator such that $m=1$, we can uniquely define the correspondence between the two systems. We use the relations,

$$\cosh(\beta\Omega) = 1 + 2\epsilon_-\epsilon_+/D, \tag{19}$$

$$D \equiv [sc(\epsilon_- - \epsilon_+)]^2, \tag{20}$$

$$2\Omega/\sinh(\beta\Omega) = D/(\epsilon_- s^2 + \epsilon_+ c^2), \tag{21}$$

$$\Omega \sinh(\beta\Omega) = \frac{2\epsilon_-\epsilon_+(1 + \epsilon_-\epsilon_+/D)}{(\epsilon_- s^2 + \epsilon_+ c^2)}, \tag{22}$$

$$\coth(\beta\Omega/2) = [\cosh(\beta\Omega) + 1]/\sinh(\beta\omega) \tag{23}$$

to obtain

$$\langle a^\dagger a\rangle = \frac{(\epsilon_- s^2 + \epsilon_+ c^2)}{4}\left(\frac{m}{\omega} + \frac{\omega}{m\epsilon_-\epsilon_+}\right). \tag{24}$$

Thus, in this passive measurement regime, in the large N limit, the occupation of the bosonic mode (which is an order parameter of the phase transition) diverges as $\epsilon_- \to 0$ when $\lambda \to \lambda_c$. In the next section we discuss the effect of this on the current measurement.

VI. POWER-LAW SCALING IN TRANSPORT PROPERTIES

A. Results

We plot the current and current noise in Figs. 2 and 4. We immediately see that, at the critical point λ_c, the large occupation of the cavity mode (which is proportional to the number of qubits N) acts to blockade the current flow (by "pushing apart" the internal energy levels of the transport qubit). Similarly, the zero-frequency noise becomes strictly Poissonian at the critical point. This is a consequence of the slow current and charge-dominated dynamics. Thus, both the current and current noise are operating as *signatures, or order parameters, of the phase transition*, because of their direct dependence on $\langle a^\dagger a\rangle$.

As mentioned earlier, in previous work[8,9] the phase transition was studied as a function of multiqubit-oscillator coupling λ. However, the transition can also be observed for a given constant λ, by tuning the energy level of the qubits ω_0. This is a more realistic approach with superconducting qubits as a possible realization. Qualitatively, the properties of the transition are the same. For instance, for $\lambda=0.1\omega$ the transition occurs when $\omega_{0,c} \to 0.04\omega$. The subradiant phase occurs for $\omega_0 > \omega_{0,c}$ while the super-radiant phase appears when $\omega_0 < \omega_{0,c}$, both of which are experimentally accessible regimes. However, because the interaction is off-resonance, the convergence to the correct scaling behavior requires much larger N.

B. Scaling with the number (N) of qubits

To observe power-law scaling with N, we must look at the derivative of both the current and current noise with respect

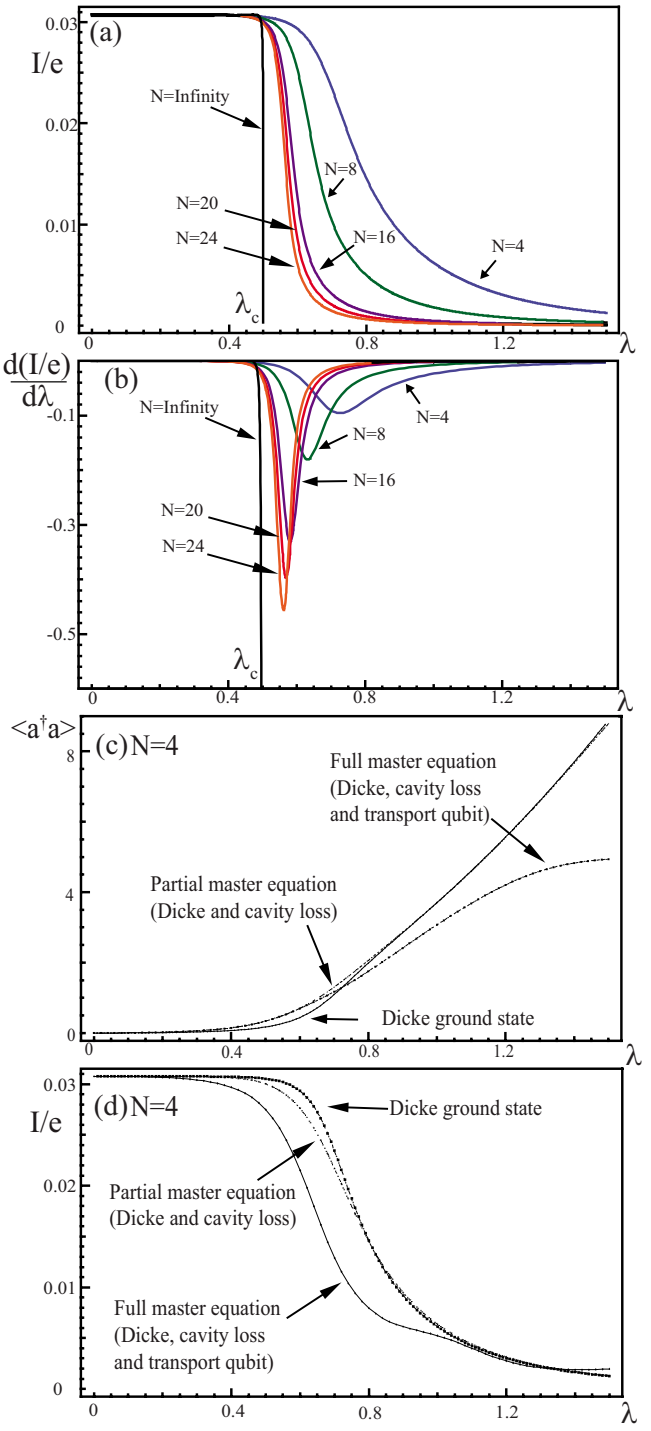

FIG. 2. (Color online) (a) The current I/e versus multiqubit-oscillator coupling λ through the transport qubit for $\Delta=0.1$, $\Gamma_L=\Gamma_R=0.1$, $\epsilon=0$, $\omega=\omega_0=1$, and $g=0.1$ for $N=4,8,16,20,24,\infty$. (b) The derivative of the current through the transport qubit for the same parameter set versus λ. (c) and (d) show one particular data curve ($N=4$, $\gamma_b=0.1$) for the bosonic occupancy $\langle a^\dagger a\rangle$ and the current I/e for the three different approximations; zero back action (ground state of the pure Dicke model), master equation with cavity damping, and master equation with cavity damping and transport qubit feedback.

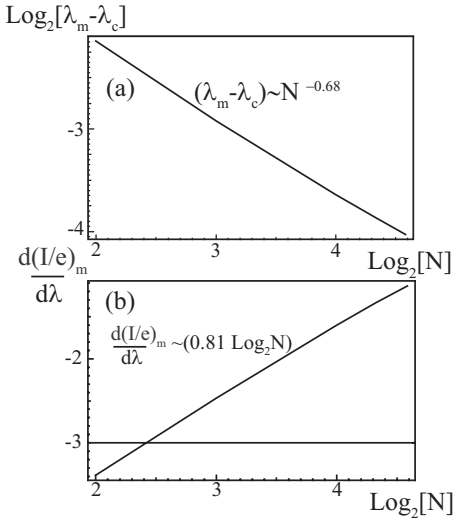

FIG. 3. (a) shows the scaling with N and scaling exponent of the position (λ_m) of the minimum of the current derivative: $(\lambda_m-\lambda_c) \propto N^{-0.68\pm0.05}$. (b) shows the scaling of the value of the current at this minimum point to be $(\frac{d(I/e)}{d\lambda})_m \propto (0.81\pm0.05)\log_2 N$. The parameters used here are $\Delta=0.1$, $\Gamma_L=\Gamma_R=0.1$, $\epsilon=0$, $\omega=\omega_0=1$, and $g=0.1$ with data taken at $N=4,8,16,20,24,40,60$.

to the Dicke multiqubit-oscillator coupling λ. The minimum value of these derivatives will act as a signature of "precursor behavior" and from them we can extract the power-law dependence. In Fig. 2(b) we show the derivative of the current and in Fig. 3(a) we see that the position of the minimum of the current derivative scales as a power law in N via

$$(\lambda_m - \lambda_c) \propto N^{-0.68\pm0.05}. \tag{25}$$

This matches a previous result for the scaling of the entanglement entropy.[7] Similarly the value of the current at this minimum point scales logarithmically as

$$\frac{d(I/e)}{d\lambda}_m \propto (0.81 \pm 0.05)\log_2 N, \tag{26}$$

as shown in Fig. 3(b). The value of the current derivative obeys similar scaling laws.

Vidal and Dusuel[31] studied the scaling, in N, at the critical point λ_c of several properties of the Dicke model. They predicted a scaling exponent for $1/\langle a^\dagger a\rangle^2$ of $\alpha=2/3$. These exponents are different from those we observe here, as they describe behavior of quantities measured exactly at λ_c. To extract the same exponents from our numerics would require very large values of N. However a recent numerical study by Chen *et al.*[34] describes a scheme where such exponents can be calculated efficiently for large N and confirmed[31] the correct exponents for some of these quantities. Their results emphasizes the point that the true scaling exponents are only visible for very large N, which may be difficult to reach for some experimental realizations.

VII. BACK ACTION AND CAVITY LOSS

To take into account both the back action of the transport qubit and the loss of photons from the cavity due to coupling to the environment, we must solve the entire master equation numerically. This is a nontrivial task, even with state-of-the-art numerics and requires careful use of sparse-matrix techniques to increase efficiency.

Dimer *et al.*[24] investigated the thermodynamic limit of the Dicke model including losses from the bosonic cavity. They found that the critical point was shifted from its normal position as a function of the cavity loss γ_b. In Figs. 2(c) and 2(d) we do the same for the finite-N case, comparing the three possible regimes: zero back action and no cavity loss, zero back action with cavity loss, and a full treatment of cavity loss and back action.

In Fig. 2(c) we see that around the critical point the occupancy of the bosonic cavity is almost exactly the same for both master-equation treatments but differs slightly from the ground-state Dicke case. Furthermore the strong-coupling limit for the full master-equation treatment saturates because of the bosonic Hilbert-space cutoff needed in solving this complex problem. Furthermore, in Fig. 2(d) we see that the full treatment of the combined transport qubit/Dicke model shows a reduced current profile compared to the two situations with zero back action. This is also the case for other values of N.

However the coupling to the qubit, and the loss of energy from the cavity, has less obvious effects on the properties of the phase transition itself. In particular, the parity,

$$\Pi = \exp[i\pi(a^\dagger a + J_z + j)] \tag{27}$$

is no longer conserved and the steady state will contain components of both the ground state and excited states of H_D. Because of this, and the restrictions on the number of spins we can efficiently model, it is not possible to extract exponents from this data. However, we expect the large-N limit to still exhibit features of the phase transition, as predicted by Dimer *et al.*[24]

VIII. SIGNATURES OF QUANTUM CHAOS

Quantum chaos is a characteristic of nonintegrable quantum systems. Emary and Brandes[9] extensively studied the (closed) Dicke model and its chaotic properties. In the finite-N regime they showed that the eigenvalue spectrum of the Dicke model fitted that of the Wigner–Dyson distribution[35] when the qubit-boson coupling was around the critical point $\lambda \approx \lambda_c$. Thus, the chaotic behavior is understood to be a "precursor" of the phase transition, driven by the parity conservation at the critical point.

Here we extend their work by identifying similar distributions in the eigenvalues,

$$\chi_i = i(E_i^L) + \nu_i \tag{28}$$

of the *Liouvillian* L which include imaginary components $i(E_i^L)$ from H_D, as well as real components ν_i from the cavity-loss terms. Here we ignore the back-action and electron-transport terms and focus on the effect of cavity damping on the level statistics.

For the pure-state case (no cavity losses), the von Neumann equation of motion,

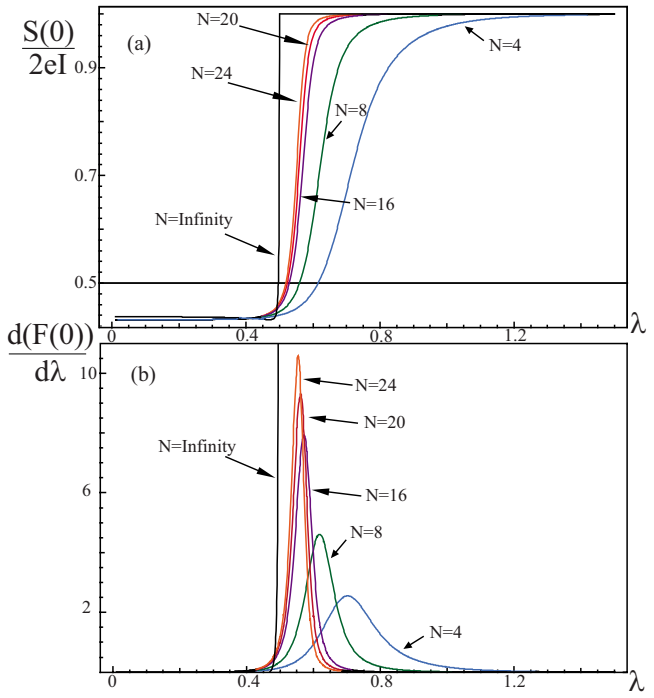

FIG. 4. (Color online) (a) The current noise $F(0)=S(0)/2eI$ versus multiqubit-oscillator coupling λ for $\Delta=0.1$, $\Gamma_L=\Gamma_R=0.01$, $\epsilon=0$, $\omega=\omega_0=1$, $g=0.1$, and for $N=4,8,16,20,24,\infty$. (b) The derivative $\frac{dF(0)}{d\lambda}$ versus λ. The peak scales as a power law of N, similar to the minimum of the current derivative.

$$\frac{\rho(t)}{dt} = -i[H,\rho(t)] \tag{29}$$

can be written as a set of N_H^2 coupled equations of the matrix elements of ρ, where N_H is the dimension of the Hilbert space for the system described by the Hamiltonian H. If H has N_H eigenvalues E_k, $k=1,\ldots,N_H$, and we take matrix elements according to the eigenbasis of H, then we can write these linear equations as a diagonal matrix with N_H^2 imaginary eigenvalues

$$E_{i=j\times k}^L = \sum_{k,j=1}^{N_H} (E_k - E_j). \tag{30}$$

Every possible energy gap (not just nearest neighbor) in the spectrum of H has an eigenvalue in L.

In Figs. 5 we show the positive branch of the imaginary components of the eigenvalues of L for $N=6$ and $\lambda=\lambda_c$, after removal of the N_H zeros, i.e., the stationary states and the probability distributions of these components. Even though it is not possible to unfold this spectrum, and all possible level spacings are present, we see some characteristics of the "picket-fence" distribution[36] of the Rabi Hamiltonian and the universal Wigner–Dyson distribution.[35]

We point out that the eigenvalues of this matrix, which is a particular representation of the superoperator L, determine many of the higher-order transport properties, like the frequency-dependent noise. This is also seen in scattering theory,[37] where there much work has been done on applying random matrix theory to transport problems. However, so far

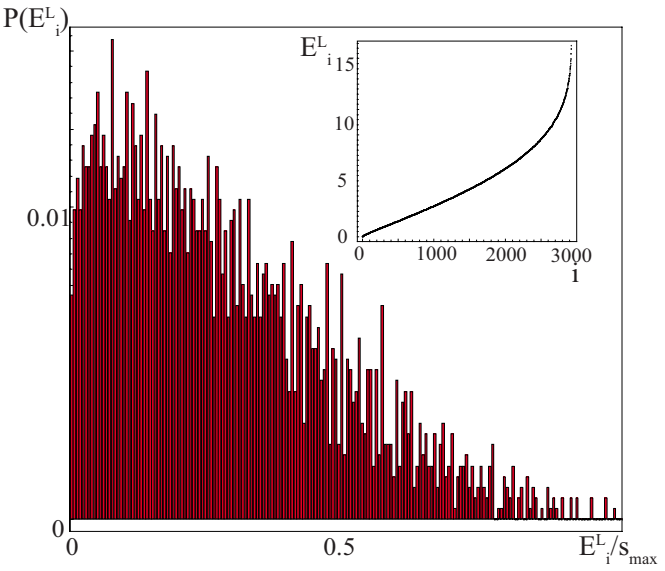

FIG. 5. (Color online) The inset shows an example of the positive imaginary components of the eigenvalues (E_i^L) of the Liouvillian for the damped Dicke model and the main figure shows their probability distribution $P(E_i^L)$, normalized to the maximum energy gap $S_{\max}$, for $N=6$, $\lambda=\lambda_c$, and $\gamma_b=0.1$. While this contains every possible eigenvalue separation of the Hamiltonian (up to numerical bosonic cutoff), and has not been unfolded to remove secular variations, level repulsion is still visible.

the application of random matrix theory to master equations[38] has been limited in scope. We hope our results will motivate readers to pursue further future studies beyond these preliminary explorations.

IX. FROM CIRCUIT QED TO THE DICKE MODEL

Al-Saidi and Stroud[39] have studied a realization of the Dicke model using Josephson junctions coupled to an electromagnetic cavity. Operating in the regime "between" charge and flux qubits they showed that, given the right parameters, the higher-lying levels of each junction can be neglected. In the same way, it is possible to derive the Dicke Hamiltonian, Eq. (1), from the Hamiltonian describing superconducting qubits interacting with a cavity. The proposal and realization of cavity QED (Refs. 10–16) in a circuit was an important development for quantum optics and condensed matter, and thus the observation of strong many-body effects in these systems is a natural extension of previous work.

Alternatively, a large number of qubits, in the form of two-level atoms in an atom chip, coupled to a transmission line, was recently proposed as a way to realize the large-N Dicke model.[22] Finally we point out a recent proposal by Mariantoni *et al.*[17,18] on coupling two resonators together via an intermediatory qubit. Such a scheme could be used to realize, experimentally, the low-coupling (normal phase) region of the Dicke model in the thermodynamic ($N\to\infty$) limit. It may also be possible to introduce more complex interactions between the two resonators, to realize other models from catastrophe theory.[40]

X. CONCLUSIONS

In conclusion, we have shown that current and current-noise measurements could be used to test for criticality in an "on chip" experiment. We extracted scaling exponents for the Dicke phase transition from semianalytical and numerical modeling, and illustrated how quantum chaos, a precursor behavior to the phase transition, is retained in an open-system environment.

ACKNOWLEDGMENTS

We thank S. Ashhab and I. Mahboob for helpful discussions. This work is supported partially by the National Science Council, Taiwan under Grant No. 95-2112-M-006-031-MY3. F.N. acknowledges partial support from the National Security Agency (NSA), Laboratory for Physical Sciences (LPS), Army Research Office (ARO), National Science Foundation (NSF) under Grant No. EIA-0130383, JSPS-RFBR under Contract No. 06-02-91200, and CTC program supported by the Japan Society for Promotion of Science (JSPS).

[1] S. Sachdev, *Quantum Phase Transitions* (Cambridge University Press, Cambridge, 1999).
[2] M. C. Gutzwiller, *Chaos in Classical and Quantum Mechanics* (Springer, Berlin, 1990).
[3] A. Osterloh, L. Amico, G. Falci, and R. Fazio, Nature (London) **416**, 608 (2002).
[4] T. J. Osborne and M. A. Nielsen, Phys. Rev. A **66**, 032110 (2002).
[5] G. Vidal, J. I. Latorre, E. Rico, and A. Kitaev, Phys. Rev. Lett. **90**, 227902 (2003).
[6] J. I. Latorre, E. Rico, and G. Vidal, Quantum Inf. Comput. **4**, 48 (2004).
[7] N. Lambert, C. Emary, and T. Brandes, Phys. Rev. Lett. **92**, 073602 (2004).
[8] K. Hepp and E. Lieb, Ann. Phys. **76**, 360 (1973).
[9] C. Emary and T. Brandes, Phys. Rev. E **67**, 066203 (2003).
[10] J. Q. You and F. Nori, Physica E (Amsterdam) **18**, 33 (2003).
[11] J. Q. You and F. Nori, Phys. Rev. B **68**, 064509 (2003).
[12] J. Q. You and F. Nori, Phys. Today **58**(11), 42 (2005).
[13] A. Wallraff, D. Schuster, A. Blais, L. Frunzio, R.-S. Huang, J. Majer, S. Kumar, S. M. Girvin, and R. J. Schoelkopf, Nature (London) **431**, 162 (2004).
[14] I. Chiorescu, P. Bertet, K. Semba, Y. Nakamura, C. J. P. M. Harmans, and J. E. Mooij, Nature (London) **431**, 159 (2004).
[15] J. Johansson, S. Saito, T. Meno, H. Nakano, M. Ueda, K. Semba, and H. Takayanagi, Phys. Rev. Lett. **96**, 127006 (2006).
[16] F. Deppe, M. Mariantoni, E. P. Menzel, A. Marx, S. Saito, K. Kakuyanagi, H. Tanaka, T. Meno, K. Semba, H. Takayanagi, E. Solano, and R. Gross, Nat. Phys. **4**, 686 (2008).
[17] M. Mariantoni, F. Deppe, A. Marx, R. Gross, F. K. Wilhelm, and E. Solano, Phys. Rev. B **78**, 104508 (2008).
[18] F. Helmer, M. Mariantoni, A. G. Fowler, J. von Delft, E. Solano, and F. Marquardt, EPL **85**, 50007 (2009).
[19] N. Lambert and F. Nori, Phys. Rev. B **78**, 214302 (2008).
[20] R. Aguado and T. Brandes, Phys. Rev. Lett. **92**, 206601 (2004).
[21] Y. M. Blanter and M. Buttiker, Phys. Rep. **336**, 1 (2000).
[22] J. Verdu, H. Zoubi, C. Koller, J. Majer, H. Ritsch, and J. Schmiedmayer, Phys. Rev. Lett. **103**, 043603 (2009).
[23] A. A. Clerk, Phys. Rev. B **70**, 245306 (2004).
[24] F. Dimer, B. Estienne, A. S. Parkins, and H. J. Carmichael, Phys. Rev. A **75**, 013804 (2007).
[25] A. A. Clerk and D. W. Utami, Phys. Rev. A **75**, 042302 (2007).
[26] J. Bourassa, J. M. Gambetta, A. A. Abdumalikov, Jr., O. Astafiev, Y. Nakamura, and A. Blais, Phys. Rev. A **80**, 032109 (2009).
[27] G. Chen, Z. Chen, and J. Liang, Phys. Rev. A **76**, 055803 (2007).
[28] J. Majer, J. M. Chow, J. M. Gambetta, J. Koch, B. R. Johnson, J. A. Schreier, L. Frunzio, D. I. Schuster, A. A. Houck, A. Wallraff, A. Blais, M. H. Devoret, S. M. Girvin, and R. J. Schoelkopf, Nature (London) **449**, 443 (2007).
[29] H. Goto and K. Ichimura, Phys. Rev. A **77**, 053811 (2008).
[30] Y. K. Wang and F. T. Hioe, Phys. Rev. A **7**, 831 (1973).
[31] J. Vidal and S. Dusuel, Europhys. Lett. **74**, 817 (2006).
[32] N. Lambert, C. Emary, and T. Brandes, Phys. Rev. A **71**, 053804 (2005).
[33] A. Blais, R.-S. Huang, A. Wallraff, S. M. Girvin, and R. J. Schoelkopf, Phys. Rev. A **69**, 062320 (2004).
[34] Q.-H. Chen, Y.-Y. Zhang, T. Liu, and K.-L. Wang, Phys. Rev. A **78**, 051801(R) (2008).
[35] T. Guhr, A. Müller-Groeling, and H. A. Weidenmüller, Phys. Rep. **299**, 189 (1998).
[36] M. Kus, Phys. Rev. Lett. **54**, 1343 (1985).
[37] C. Beenakker, Rev. Mod. Phys. **69**, 731 (1997).
[38] C. Timm, arXiv:0905.2859 (unpublished).
[39] W. A. Al-Saidi and D. Stroud, Phys. Rev. B **65**, 224512 (2002).
[40] C. Emary, N. Lambert, and T. Brandes, Phys. Rev. A **71**, 062302 (2005).